Chiral Films

Deutsche Ausgabe: DOI: 10.1002/ange.201500277
Internationale Ausgabe: DOI: 10.1002/anie.201500277

Coassembly of Nanorods and Nanospheres in Suspensions and in Stratified Films**

*Héloïse Thérien-Aubin, Ariella Lukach, Natalie Pitch, and Eugenia Kumacheva**

Abstract: *The entropically driven coassembly of nanorods (cellulose nanocrystals, CNCs) and nanospheres (dye-labeled spherical latex nanoparticles, NPs) was studied in aqueous suspensions and in solid films. In mixed CNC-latex suspensions, phase separation into an isotropic latex-NP-rich and a chiral nematic CNC-rich phase took place; the latter contained a significant amount of latex NPs. Drying the mixed suspension resulted in CNC-latex films with planar disordered layers of latex NPs, which alternated with chiral nematic CNC-rich regions. In addition, fluorescent latex NPs were embedded in the chiral nematic domains. The stratified morphology of the films, together with a random distribution of latex NPs in the anisotropic phase, led to the films having close-to-uniform fluorescence, birefringence, and circular dichroism properties.*

Coassembly of nanoparticles (NPs) with distinct shape-, size-, and composition-dependent properties is a promising approach for the preparation of multicomponent nanostructured materials with new or enhanced properties.[1–4] To form a material with a desired nanostructure, fundamental understanding has to be developed about the governing principles of the coassembly process. For example, the structure of linear chains assembled from different types of plasmonic NPs depends on the relationship between the rate of self-assembly of each individual component and the rate of coassembly.[5,6] Alternatively, one of the components can function as a template for the spatial organization of the second one.[7] A particularly interesting case is entropically mediated coassembly of NPs with different shapes, for example, nanorods and nanospheres. These systems exhibit a variety of structures, including macroscopic demixing of rods and spheres as well as microscopic and nanoscopic phase separation into layers of rods alternating with layers of spheres.[8,9] Although nematic and smectic phases of side-by-side assembled rods have been studied, the coassembly of spheres and rods that organize in chiral nematic (N*) phases has not been reported. Such structures show chiral optical properties, and thus, in addition to microscopy, the structure of the coassembled system can be examined by measuring its circular dichroism.

A beautiful example of nanorods organizing in N* structures are cellulose nanocrystals (CNCs). The chiral nematic organization of CNCs occurs in aqueous suspensions at a sufficiently high CNC concentration.[10,11] Although overwhelming experimental evidence exists for the N* order in CNC suspensions and films,[10–14] the origin of this effect is a subject of debate.[15–19] It has been suggested that the N* nature of CNC mesophases can be caused by the transfer of the chirality from the glucose units to the cellulose molecules and to the CNCs,[15] through a twist along the long axis of the CNCs[16,17] or by the fact that the charges on the CNC surface adopt a threaded screw distribution.[18,19]

The N* order is preserved in solid CNC films obtained by evaporation of water from CNC suspensions, and as a result, the CNC films exhibit iridescence, tunable color, and chiroptical activity.[10] The properties of the CNC films can be tuned by the use of additives[20] and by controlling the processing conditions.[21,22] The coassembly of CNCs with small (typically, not exceeding several percent) volume fractions of metal,[23,24] semiconductor,[25] or magnetic[26] NPs yielded films with combined photonic and chiroptical properties of the CNC host and plasmonic, luminescence, and magnetic properties of the NPs, however structural characterization of the coassembled structures of CNCs and spherical NPs has not been reported.

Herein we report the coassembly of high aspect ratio CNCs with spherical latex NPs. Such systems, in addition to their fundamentally interesting behavior, may have important applications. A significant enhancement in the mechanical properties of the composite films derived from CNC-latex mixtures can be readily achieved by tuning the composition of the latex NPs by copolymerization of appropriate monomers. Moreover, although composite films of CNCs and hydrophobic polymers are generally derived from organogels[27] or by dispersing lyophilized CNCs in apolar media,[28] the use of latex NPs maintains the system water-borne. Until now, in the CNC-latex mixtures studied, CNCs were added as a minor phase and acted as a reinforcing agent.[29,30] Under these conditions, the ability of the CNCs to assemble into an N* structure and the corresponding optical properties of the

[*] H. Thérien-Aubin,[+] A. Lukach,[+] N. Pitch, Prof. E. Kumacheva
Department of Chemistry, University of Toronto
80 St. George Street, Toronto, M5S 3H6 (Canada)
E-mail: ekumache@chem.utoronto.ca
Prof. E. Kumacheva
Department of Chemical Engineering and Applied Chemistry
University of Toronto, 200 College Street, Toronto
Ontario M5S 3E5, Canada
Prof. E. Kumacheva
The Institute of Biomaterials and Biomedical Engineering
University of Toronto, 4 Taddle Creek Road, Toronto
Ontario M5S 3G9, Canada
[+] These authors contributed equally to this work.

[**] We thank the NSERC Canada for financial support, Prof. Ron Kluger for the use of the CD spectropolarimeter and Ilya Gourevich (the Center of Nanostructure Imaging) for assistance with electron microscopy experiments.
Supporting information for this article is available on the WWW under http://dx.doi.org/10.1002/anie.201500277.

composite films were not realized.[4] Instead, the CNCs formed a percolation network in the disordered latex phase.

Herein, we studied the coassembly of CNCs and solid latex NPs that were mixed in comparable volume fractions. The latex NPs were labeled with a fluorescent dye. Coassembly was studied in mixed CNC-latex suspensions and in solid films. In addition to microscopy studies of the structure of the mixed suspensions and films, we examined the macroscopic properties of the CNC-latex mixtures by circular dichroism (CD) and fluorescence, which were governed by the organization of the CNCs and latex NPs, respectively, in the films. In contrast to earlier studies on CNC-latex mixtures, we observed the formation of two types of structures. Micrometer-thick CNC-rich layers with a chiral nematic structure alternated with disordered latex-rich layers. These layers were aligned in the plane of the film. In addition to microscopic layering, a significant fraction of the latex NPs was distributed in the N* regions of the CNC matrix.

As a consequence of the stratified planar structure and random distribution of the latex NPs in the N* phase, the CNC-latex films exhibited close-to-uniform macroscopic properties, namely, CD and birefringence, both characteristic of the CNC matrix, and the fluorescence properties of the latex NPs. Thus the entropically driven coassembly of the CNC matrix with latex NPs offered a new approach to nanocomposite materials by combining the macroscopic properties of the individual components.

Dye-labeled poly(ethyl methacrylate) latex NPs with a mean diameter of (154 ± 30) nm, glass transition temperature of 68 °C, and electrokinetic potential (ζ-potential) of (-46 ± 8) mV were synthesized by emulsion copolymerization of ethyl methacrylate and 9-vinylanthracene. High aspect ratio rodlike anionic CNCs derived from wood pulp by acid hydrolysis[31] had a mean diameter and length of (13 ± 4) and (180 ± 70) nm, respectively, and a ζ-potential of (-47 ± 10) mV. Scanning electron microscopy (SEM) images of the CNCs and latex NPs are shown in Figure 1 a,b, respectively. The coassembled films of the CNCs and latex NPs were prepared by mixing their aqueous suspensions and subsequent drying of the mixtures at 85–90 % relative humidity and 25 °C, that is, below the glass transition temperature of the latex NPs. The latex weight fraction in the dry films was up to 50 wt % (corresponding to a volume fraction, ϕ_{latex}, of 0.57). Latex-free CNC suspensions and films at $\phi_{latex} = 0$ were used as control systems.

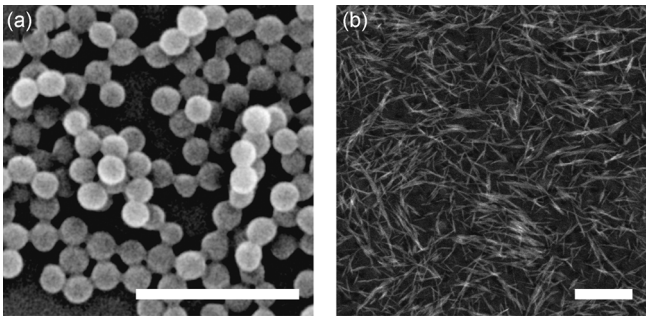

Figure 1. Scanning electron microscopy images of poly(ethyl methacrylate) latex NPs (a) and CNCs (b). Scale bars are 500 nm.

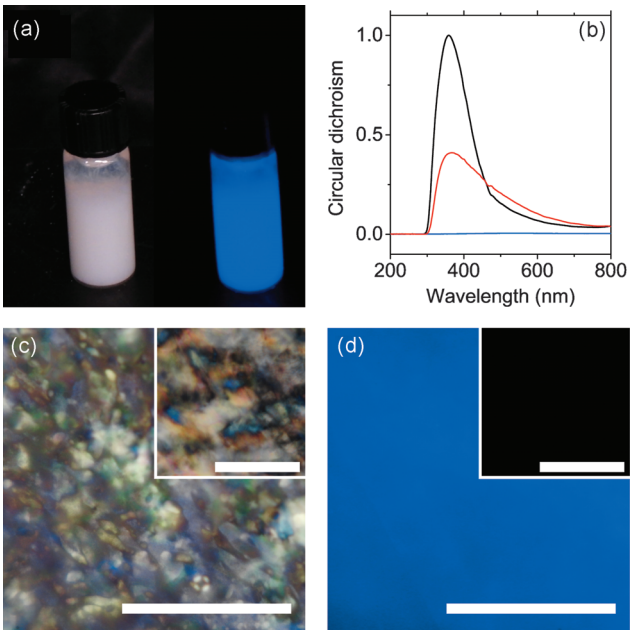

Figure 2. a) A photograph of the CNC-latex suspension ($\phi_{latex} = 0.31$) illuminated with white light (left) and UV light at $\lambda = 365$ nm (right). The volume ratio of latex-NPs-to-CNCs is 0.44:1 (corresponding to $\phi_{latex} = 0.31$ in the film). b) Circular dichroism spectra of the coassembled CNC-latex films with $\phi_{latex} = 0$ (black), $\phi_{latex} = 0.31$ (red), and $\phi_{latex} = 0.57$ (blue). c) Polarization optical microscopy image and d) optical fluorescence microscopy image of the CNC-latex film with $\phi_{latex} = 0.31$. In (c) and (d), the insets show the corresponding images of a latex-free CNC film ($\phi_{latex} = 0$). Scale bars are 250 μm.

Equilibration of the sealed mixed CNC-latex suspensions for 24 h led to their phase separation into an anisotropic N* phase (top) and an isotropic phase (bottom; Figure 2 a). Importantly, the latex NPs partitioned in both phases, as evident from the fluorescence emission of the anthracene fluorophore. Autofluorescence of the CNCs was ruled out, since latex-free phase-separated suspensions of CNCs did not exhibit fluorescence under these conditions (see Figure S2 in the Supporting Information).[32] Moreover, by conducting extensive dialysis of the latex dispersion prior to coassembly experiments, we ensured that free dye was not present in the system (see Figure S3 in the Supporting Information).

The chiroptical activity of the coassembled films was studied by CD spectroscopy. The CD spectrum of the latex-free N* film (Figure 2 b, black spectrum) showed a strong positive signal arising from the selective transmission of right-handed circularly polarized light by the left-handed helical structure of the CNCs.[33] The CD properties were preserved in the CNC-latex films with $\phi_{latex} = 0.31$ (Figure 2 b, red spectrum), although the full-width at half-maximum of the CD peak notably increased, which indicates a broader distribution of the N* pitch values. The 57 % reduction of the CD signal in the coassembled films was ascribed to a combination of a reduced CNC fraction in the films and partial disruption of the N* order. The position of the maximum of the CD peak remained invariant, thus suggesting that the properties of the remaining N* domains were not significantly affected by the presence of the latex NPs. The CD signal drastically reduced at $\phi_{latex} = 0.57$ (Figure 2 b, blue

spectrum), which suggests a strong disruption of the N* order in the coassembled CNC-latex films. Therefore, further structural studies were performed on the CNC-latex suspensions and films with $\phi_{latex} = 0.31$.

The existence of the N* structure in the CNC-latex films was also established in polarization optical microscopy (POM) experiments. The coassembled films displayed a marble-like texture, typical of N* order (Figure 2c),[34] similar to the latex-free CNC film (Figure 2c, inset). The distribution of latex NPs in the films was examined in optical fluorescence microscopy experiments. Composite films exhibited macroscopically (over a millimeter scale) uniform fluorescence, with less than 3% variation in intensity (Figure 2d). In contrast, latex-free CNC films appeared black under illumination at $\lambda = 365$ nm (Figure 2d, inset). The macroscopically uniform birefringence texture and fluorescence suggested that although the latex NPs were distributed throughout the films on a macroscopic scale, their presence did not disrupt the N* order of the CNC matrix.

Since the structure of the composite films is largely determined by the structure of the corresponding suspension (prior to film casting), phase separation was examined in CNC-latex suspensions with $\phi_{latex} = 0.31$ (and compared with a suspension at $\phi_{latex} = 0$). The suspensions were introduced into a 100 μm thick cell and equilibrated for 3 days. In both systems, phase separation between the N* phase (droplets characterized by a typical fingerprint texture) and an isotropic phase (appearing black in POM images)[32] were observed, although the N* droplets became more scarce in the mixed suspension (Figure 3a,b). Measurement of the distance between adjacent lines of the fingerprint texture revealed that the half-pitch of the N* domains (the distance over which the nematic order undergoes half a turn, see Figure S4 in the Supporting Information)[32] increased from (14 ± 3) μm in the latex-free CNC suspension to (24 ± 10) μm in the CNC-latex suspension (Figure 3c,d, respectively), in agreement with pitch values reported for dilute suspensions of wood-based CNCs.[35] Spatial variation in the fluorescence intensity in the latex-free CNC suspension and in the CNC-latex suspension (Figure 3e,f, respectively) was examined within the corresponding areas imaged by POM (Figure 3c,d, respectively). Fluorescence from the anthracene-labeled NPs was observed both outside and inside the N* droplets (Figure 3f). The fluorescence intensity in the N* regions was (30 ± 10)% lower than in the isotropic phase (see Figure S5 in the Supporting Information), which indicates that the latex NPs partitioned in both phases, albeit at a lower concentration in the N* domains.

The structure of the coassembled CNC-latex films was characterized by SEM imaging of the cross-section of the film. Cross-sections of the latex-free CNC films were imaged for comparison (see Figure S8 in Supporting Information for the corresponding SEM images as well as Figures S9 and S10a for a schematic representation of the film structure).

A low magnification image (Figure 4a) of the CNC-latex films exhibited a layered structure. Inspection of the film structure at higher magnification (Figure 4b) revealed the layering occurred in microscopic CNC-rich regions (lighter domains with vertical stripes) and latex-rich "islands" (darker regions). The randomly packed latex-rich regions were (5 ± 4) μm thick and (30 ± 25) μm long, forming layers in the plane of the film. The latex-rich regions formed (19 ± 10)% of the cross-section of the CNC-latex films, measured as a fraction of the surface area of latex-rich domains (see Figure S11 in the Supporting Information).

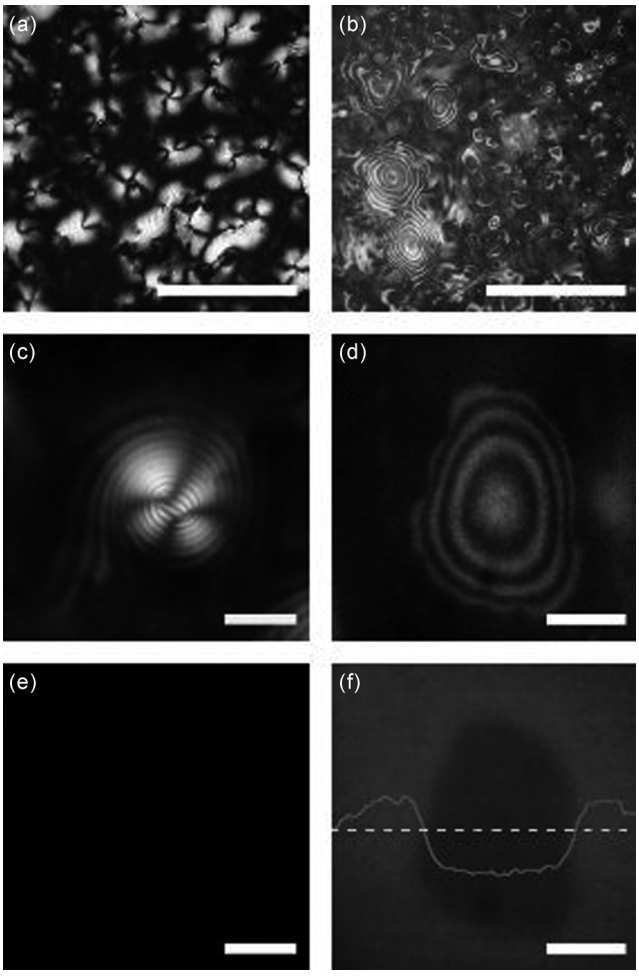

Figure 3. Latex-free CNC and composite CNC-latex suspensions. Polarized optical microscopy images (a–d) and fluorescence microscopy images (e,f) of the latex-free CNC suspension (a,c,e) and CNC-latex suspension at $\phi_{latex} = 0.31$ (b,d,f). The scale bars are 250 μm in (a,b) and 100 μm in (c–f). The line in (f) is the fluorescence intensity profile along the dashed line. Approximately 10 images were used to measure the N* pitch and the fluorescence intensity.

The layered periodic structure of the CNC-rich regions (Figure 4b,c and see Figure S7 in the Supporting Information) was characteristic of the N* order.[12] During film preparation by drying a mixed suspension, the pitch of the N* phase decreased from 48 μm to (220 ± 80) nm in the film (in the latex-free CNC films the pitch was 220 ± 60 nm; see Figure S8 in the Supporting Information). A fraction of the latex NPs was compartmentalized within the CNC-rich N* regions (Figure 4c,d and see Figures S6 and S7 in the Supporting Information), consistent with their inclusion in the N* phase in the CNC-latex suspensions.

Figure 5 illustrates schematically the organization of the CNCs and latex NPs in suspensions (Figure 5a–c) and in stratified films. Partial demixing took place in the liquid

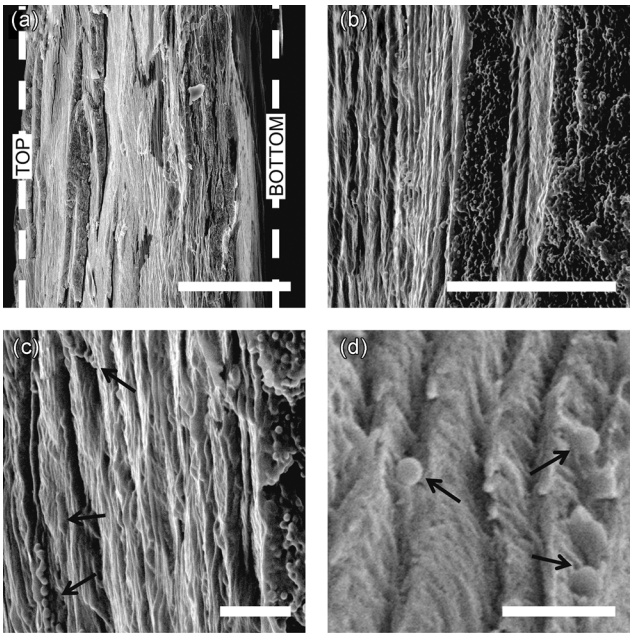

Figure 4. Scanning electron microscopy images of the cross-section of films with $\phi_{latex} = 0.31$. The scale bars are a) 10 μm, b) 5 μm, c) 1 μm, and d) 500 nm. In (a) the dashed lines represent the borders of the film. In (b) the lighter striped region corresponds to the CNC-rich phase and the darker region corresponds to the latex-NP-rich phase. In (c,d) the black arrows point to latex NPs embedded in the chiral nematic domains.

phase, (Figure 5c), thereby leading to the coexistence of a latex-rich disordered phase and a CNC-rich N* phase. Following evaporation of water from the mixed suspension, the N* order was largely preserved in the CNC-rich regions in solid films, which alternated with latex-NP-rich disordered domains.

It is currently established, both experimentally and theoretically, that rodlike colloidal particles, for example, inorganic nanorods[37,38] or tobacco mosaic virus,[38–40] form nematic structures as a consequence of the gain in translational entropy, which for aligned rods increases because of favored excluded volume interactions, thereby compensating for the loss in orientational entropy of the system.[41]

In a binary mixture of rods and spheres and in the absence of electrostatic attraction between them, particle geometry governs their interactions.[9] The phase separation between the sphere-rich and rod-rich phases takes place in a liquid state, and at a high volume fraction of spheres, the existence of a single isotropic phase is predicted.[42] This effect was observed in our study on the CNC-latex mixture at $\phi_{latex} = 0.57$. At a lower content of spheres, the demixing of two equilibrium phases is predicted: a nematic phase rich in rods and an isotropic sphere-rich phase.[42] In our study, we observed microscopic phase separation at $\phi_{latex} = 0.31$. It should be stressed, however, that in our study the rodlike CNCs exhibited a N* organization, in contrast to existing predictions made for the formation of nematic rod-rich phases.[42] Sphere-rod demixing and ordering in such systems may show additional complexity and has not been explored, either experimentally or theoretically.

The formation of latex-rich islands in the CNC-latex films was ascribed to excluded volume interactions leading to depletion forces between the latex NPs. The addition of small colloids to a suspension of larger particles can induce flocculation of the larger particles, because of depletion attraction between them.[43,44] In our study, the latex NPs had a significantly larger volume than the CNCs, and could experience attraction in the presence of CNCs. As a result of geometric constraints,[45,46] attraction parallel to the stratified N* structure was favored, thereby leading to the formation of the elongated islands of randomly packed latex NPs. The N* organization of the CNCs resulted in the demixed latex-NP-rich regions forming layers in the plane of the film (Figure 5d), as confirmed by the fluorescence and SEM imaging results (Figures 3f and 4). Such a stratified morphology of the films, together with a random distribution of fluorescent latex NPs in the N* phase, provided a close-to-uniform fluorescence and preserved the CD properties of the films.

In conclusion, we have shown that the entropically driven coassembly of high aspect ratio rodlike CNCs and spherical latex NPs yields suspensions that exhibit chiral nematic order, with the latex NPs partitioned in both the isotropic phase and the anisotropic N* domains. Upon drying, these suspensions form films that preserve the long-range N* order of the CNC-rich phase and exhibit a stratified morphology, with latex-rich layers and CNC-rich N* layers, with latex NPs included in the N* layer. Layering of the latex NP-rich and CNC-rich phases resulted in apparently homogeneous macroscopic properties of the composite films such as fluorescence, birefringence, and CD. This structure and the properties of the composite

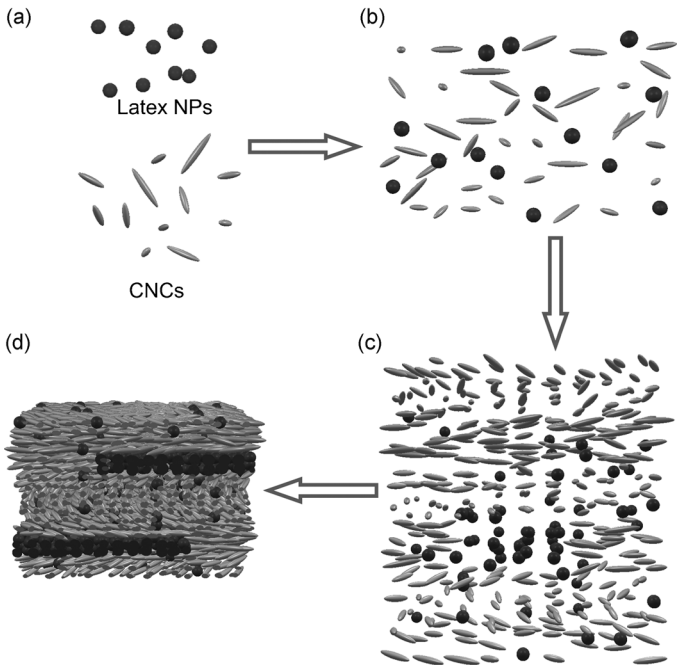

Figure 5. Schematic illustration of the coassembly of CNC-latex NP suspensions and films. a) Individual suspensions of CNCs and latex NPs; b) CNC-latex suspension; c) phase separation in a CNC-latex suspension, leading to the formation of an N* phase and an isotropic phase (not shown), both containing latex NPs. d) Stratified CNC-latex film containing latex NP-rich and CNC-rich N* regions.

films made from CNCs (rod-shape particles) and latex NPs (spherical particles) is important for their future applications as sensors and polarizers, as well as for coatings with enhanced mechanical properties.

Experimental Section

Latex synthesis: A semicontinuous "seed-and-feed" process was used for the synthesis of ≈150 nm diameter latex NPs. In the first step of the semicontinuous process, ethyl methacrylate (EtMA, 3.5 mL) was emulsified in water (55 mL) containing sodium dodecylsulfate (SDS, 12.5 mg). The suspension was heated to 80 °C and purged with N_2 gas for 30 min. A solution of potassium persulfate (KPS, 60 mg) in deionized water (5 mL) was injected using a metering pump to the suspension at a rate of 0.5 mL min^{-1} under stirring at 200 rpm by a mechanical stirrer. After 1 h of polymerization, a solution of vinylanthracene (100 mg) in EtMA (30 mL) and a solution of KPS (40 mg) and SDS (37.5 mg) in water (25 mL) were injected into the flask by using two metering pumps at a rate of 0.3 and 0.25 mL min^{-1}, respectively. After 20 h, the polymerization was stopped, and the latex dispersion was purified by dialysis over one week, with the water changed every day.

Film preparation: Individual suspensions of CNCs and latex NPs, both with a concentration of 2.5 wt%, were prepared. Mixed suspensions of CNCs and latex NPs were prepared by mixing the CNC suspension (1.5 mL) and latex suspension (0.5 mL). A mixed suspension (2 mL) was cast in a 2.21 cm plate containing either a round glass slide (18 × 0.2 mm) or a Si wafer (15 × 15 × 0.5 mm). The suspension was dried for 1 week at ≈25 °C and 85–90% relative humidity.

Phase separation in suspension: To study the phase separation in mixed suspensions, a CNC-latex suspension was introduced in a 100 μm thick cell, sealed, and equilibrated for 3 days.

Keywords: cellulose nanocrystals · chiral films · nanoparticles · self-assembly

How to cite: *Angew. Chem. Int. Ed.* **2015**, *54*, 5618–5622
Angew. Chem. **2015**, *127*, 5710–5714

[1] M. A. S. Azizi Samir, F. Alloin, A. Dufresne, *Biomacromolecules* **2005**, *6*, 612–626.
[2] O. D. Velev, S. Gupta, *Adv. Mater.* **2009**, *21*, 1897–1905.
[3] S. Singamaneni, V. V. Tsukruk, *Soft Matter* **2010**, *6*, 5681–5692.
[4] K. Hu, D. D. Kulkarni, I. Choi, V. V. Tsukruk, *Prog. Polym. Sci.* **2014**, *39*, 1934–1972.
[5] K. Liu, A. Lukach, K. Sugikawa, S. Chung, J. Vickery, H. Therien-Aubin, B. Yang, M. Rubinstein, E. Kumacheva, *Angew. Chem. Int. Ed.* **2014**, *53*, 2648–2653; *Angew. Chem.* **2014**, *126*, 2686–2691.
[6] L. J. Hill, N. E. Richey, Y. Sung, P. T. Dirlam, J. J. Griebel, E. Lavoie-Higgins, I.-B. Shim, N. Pinna, M.-G. Willinger, W. Vogel, J. J. Benkoski, K. Char, J. Pyun, *ACS Nano* **2014**, *8*, 3272–3284.
[7] M. Grzelczak, J. Vermant, E. M. Furst, L. M. Liz-Marzán, *ACS Nano* **2010**, *4*, 3591–3605.
[8] M. Adams, Z. Dogic, S. L. Keller, S. Fraden, *Nature* **1998**, *393*, 349–352.
[9] X. Ye, J. A. Millan, M. Engel, J. Chen, B. T. Diroll, S. C. Glotzer, C. B. Murray, *Nano Lett.* **2013**, *13*, 4980–4988.
[10] J. F. Revol, L. Godbout, D. G. Gray, *J. Pulp Pap. Sci.* **1998**, *24*, 146–149.
[11] I. Hoeger, O. J. Rojas, K. Efimenko, O. D. Velev, S. S. Kelley, *Soft Matter* **2011**, *7*, 1957–1967.
[12] J. Majoinen, E. Kontturi, O. Ikkala, D. G. Gray, *Cellulose* **2012**, *19*, 1599–1605.
[13] A. G. Dumanli, H. M. van der Kooij, G. Kamita, E. Reisner, J. J. Baumberg, U. Steiner, S. Vignolini, *ACS Appl. Mater. Interfaces* **2014**, *6*, 12302–12306.
[14] D. G. Gray, *J.-For.* **2013**, *3*, 6–8
[15] J. H. Park, J. Noh, C. Schütz, G. Salazar-Alvarez, G. Scalia, L. Bergström, J. P. F. Lagerwall, *ChemPhysChem* **2014**, *15*, 1477–1484.
[16] J. Araki, S. Kuga, *Langmuir* **2001**, *17*, 4493–4496.
[17] K. Fleming, D. G. Gray, S. Matthews, *Chem. Eur. J.* **2001**, *7*, 1831–1836.
[18] M. Khandelwal, A. Windle, *Carbohydr. Polym.* **2014**, *106*, 128–131.
[19] W. J. Orts, L. Godbout, R. H. Marchessault, J. F. Revol, *Macromolecules* **1998**, *31*, 5717–5725.
[20] X. Mu, D. G. Gray, *Langmuir* **2014**, *30*, 9256–9260.
[21] S. Beck, J. Bouchard, G. Chauve, R. Berry, *Cellulose* **2013**, *20*, 1401–1411.
[22] E. D. Cranston, D. G. Gray, *Colloids Surf. A* **2008**, *325*, 44–51.
[23] A. Querejeta-Fernández, G. Chauve, M. Methot, J. Bouchard, E. Kumacheva, *J. Am. Chem. Soc.* **2014**, *136*, 4788–4793.
[24] Q. Liu, M. G. Campbell, J. S. Evans, I. I. Smalyukh, *Adv. Mater.* **2014**, *26*, 7178–7184.
[25] T.-D. Nguyen, W. Y. Hamad, M. J. MacLachlan, *Adv. Funct. Mater.* **2014**, *24*, 777–783.
[26] T. Nypelö, C. Rodriguez-Abreu, J. Rivas, M. Dickey, O. Rojas, *Cellulose* **2014**, *21*, 2557–2566.
[27] J. R. Capadona, O. Van Den Berg, L. A. Capadona, M. Schroeter, S. J. Rowan, D. J. Tyler, C. Weder, *Nat. Nanotechnol.* **2007**, *2*, 765–769.
[28] K. Ben Azouz, E. C. Ramires, W. Van den Fonteyne, N. El Kissi, A. Dufresne, *ACS Macro Lett.* **2012**, *1*, 236–240.
[29] V. Favier, H. Chanzy, J. Y. Cavaille, *Macromolecules* **1995**, *28*, 6365–6367.
[30] L. Chazeau, J. Y. Cavaillé, G. Canova, R. Dendievel, B. Boutherin, *J. Appl. Polym. Sci.* **1999**, *71*, 1797–1808.
[31] X. Dong, J.-F. Revol, D. Gray, *Cellulose* **1998**, *5*, 19–32.
[32] J. F. Revol, H. Bradford, J. Giasson, R. H. Marchessault, D. G. Gray, *Int. J. Biol. Macromol.* **1992**, *14*, 170–172.
[33] J. P. F. Lagerwall, C. Schutz, M. Salajkova, J. Noh, J. Hyun Park, G. Scalia, L. Bergstrom, *NPG Asia Mater.* **2014**, *6*, e80.
[34] P. J. Collings, M. Hird, *Introduction to Liquid Crystals: Chemistry and Physics*, Taylor & Francis, London, **1997**.
[35] Y. Habibi, L. A. Lucia, O. J. Rojas, *Chem. Rev.* **2010**, *110*, 3479–3500.
[36] X. Huang, S. Neretina, M. A. El-Sayed, *Adv. Mater.* **2009**, *21*, 4880–4910.
[37] D. V. Talapin, E. V. Shevchenko, C. B. Murray, A. Kornowski, S. Förster, H. Weller, *J. Am. Chem. Soc.* **2004**, *126*, 12984–12988.
[38] S. Fraden, G. Maret, D. L. D. Caspar, R. B. Meyer, *Phys. Rev. Lett.* **1989**, *63*, 2068–2071.
[39] V. A. Parsegian, S. L. Brenner, *Nature* **1976**, *259*, 632–635.
[40] S. Fraden, G. Maret, D. L. D. Caspar, *Phys. Rev. E* **1993**, *48*, 2816–2837.
[41] L. Onsager, *Ann. N. Y. Acad. Sci.* **1949**, *51*, 627–659.
[42] A. Cuetos, B. Martínez-Haya, S. Lago, L. F. Rull, *Phys. Rev. E* **2007**, *75*, 061701.
[43] V. J. Anderson, H. N. W. Lekkerkerker, *Nature* **2002**, *416*, 811–815.
[44] S. Asakura, F. Oosawa, *J. Chem. Phys.* **1954**, *22*, 1255–1256.
[45] F. Mondiot, R. Botet, P. Snabre, O. Mondain-Monval, J.-C. Loudet, *Proc. Natl. Acad. Sci. USA* **2014**, *111*, 5831–5836.
[46] P. van der Schoot, *J. Chem. Phys.* **2000**, *112*, 9132–9138.

Received: January 12, 2015
Published online: March 16, 2015

